

Two-dimensional structures formed in a binary system of DNA nanoparticles with a short-range interaction potential

メタデータ	言語: eng 出版者: 公開日: 2018-11-09 キーワード (Ja): キーワード (En): 作成者: メールアドレス: 所属:
URL	https://doi.org/10.24517/00052743

This work is licensed under a Creative Commons Attribution-NonCommercial-ShareAlike 3.0 International License.



Two-dimensional structures formed in a binary system of DNA nanoparticles with a short-range interaction potential

Masahide Sato

Information Media Center, Kanazawa University, Kanazawa 920-1192, Japan

Covering nanoparticles with DNA strands is one of the useful methods of controlling the interaction between particles because DNA strands can be easily designed according to our specifications. Obtaining an idea from the two-dimensional structures formed by the nanoparticles covered with DNA strands, which we call DNA nanoparticles, we carry out Brownian dynamics simulations and study the formation of two-dimensional structures in a binary system. We assume that the different types of particles attract each other with Morse potential, which is minimum when their distance is σ' . When the types of particles are the same and their distance is smaller than σ , the particles are repulsive. The mixture of both square and triangular lattices is formed when $\sigma'/\sigma = 1$. With decreasing σ'/σ , a square lattice, a honeycomb lattice, and string-shaped clusters are formed. The coexistence of both square and triangular lattices with large σ'/σ and the formation of stringlike clusters with small σ'/σ occur because we neglect the attraction between the same types of particles and use a short-range attraction between different types of particles.

1. Introduction

Covering nanoparticles with DNA strands is one of the useful methods of controlling the interaction between particles because DNA strands can be easily designed as we desire. By selecting linkers, the DNA strands covering two types of nanoparticles,¹⁻⁶⁾ and the shapes of nanoparticles,⁷⁻⁹⁾ many types of three-dimensional lattice structures can be formed. These nanoparticles covered with DNA strands are expected to be potential materials for various applications, for example, medical diagnostics,¹⁰⁾ flash memories,¹¹⁾ and plasmonic materials.¹²⁻¹⁵⁾

Recently, a few groups¹⁶⁻¹⁸⁾ have succeeded in forming two-dimensional lattice structures on a lipid layer in solution of a binary system of nanoparticles covered with DNA strands, which we call DNA nanoparticles. In Ref. 16, the authors observed that the two-dimensional structure on a lipid interface is changed from a triangular lattice to an amorphous structure via stringlike clusters when the salt concentration in the solution increases. Assuming that the decrease in the length of DNA chains with increasing salt

concentration causes the increase in the connectivity of complementary particles and induces the spontaneous breaking of symmetric interactions, they carried out Monte Carlo simulations and showed that the collective behavior of DNA chains and their flexibility play important roles in the transition in the two-dimensional structure.

In Refs. 17 and 18, the authors showed that both the lattice structure and lattice constant are changed by adjusting the density of magnesium ions in solution. The magnesium ions affect DNA structures in solution:^{19,20)} the magnesium ions shrink the single-stranded DNA²¹⁾ and thermally stabilize the double-stranded DNA.^{22,23)} Thus, we expect that the change in the density of magnesium ions affects the interaction between DNA nanoparticles. In Ref. 18, a triangular lattice changed a square lattice and the lattice constant decreased with increasing magnesium ion density.

We consider that there are at least two types of approaches to study the structures formed by DNA nanoparticles in simulation. One is to use a coarse-grained model formed by particles covered with the chains of beads,²⁴⁻²⁷⁾ which represent DNA strands. The other is to consider the effective interaction potential between two particles such as a soft-core potential,²⁸⁻³⁰⁾ a square-well potential,³¹⁾ and a core-corona potential.³²⁻³⁵⁾ In our previous papers,^{36,37)} we obtained an idea from experiments^{17,18)} and studied the formation of two-dimensional structures using the Lennard-Jones (LJ) potential as the interaction potential $U(r)$, where r is the distance between two particles. We assumed that $U(\sigma) = 0$ when the types of two particles are the same and $U(\sigma') = 0$ when the types of two particles are different. We studied how the two-dimensional structures formed in a binary system depend on σ'/σ . In our simulation,³⁶⁾ a triangular lattice is formed when $\sigma'/\sigma = 1$, and a square lattice, a honeycomb lattice, and a rectangular lattice are formed with decreasing σ'/σ .

The LJ potential is a simple potential but its interaction range is sufficiently long for particles to interact with the second nearest neighbors when σ'/σ is small. The effect of the second nearest neighbors on the structures formed in our previous model³⁶⁾ is unclear. Since the attraction used in that model acts when the types of particles are not only different but also the same, the role of the attraction between the same type of particles for the formation of structures is also unclear. Thus, we study the formation of two-dimensional structures using another interaction potential with a short-range attraction.

In this paper, we use a modified Morse potential and carry out Brownian dynamics simulations to study two-dimensional structures in a binary system. We assume that

particles are attractive when their types are different and repulsive when their types are the same. Comparing our results with Ref. 36, we clarify the role of the attraction between the same type of particles and the effect of the range of attraction on the formation of two-dimensional structures. In Sect. 2, we show our model. We assume that the potential for the different types of particles is minimum when the distance between the particles is σ and the same types of particles are repulsive when the distance between them is smaller than σ . In Sect. 3, we show our results. We carry out Brownian dynamics simulations and study the relationship between two-dimensional structures and σ'/σ . In Sect. 4, we summarize our results.

2. Model

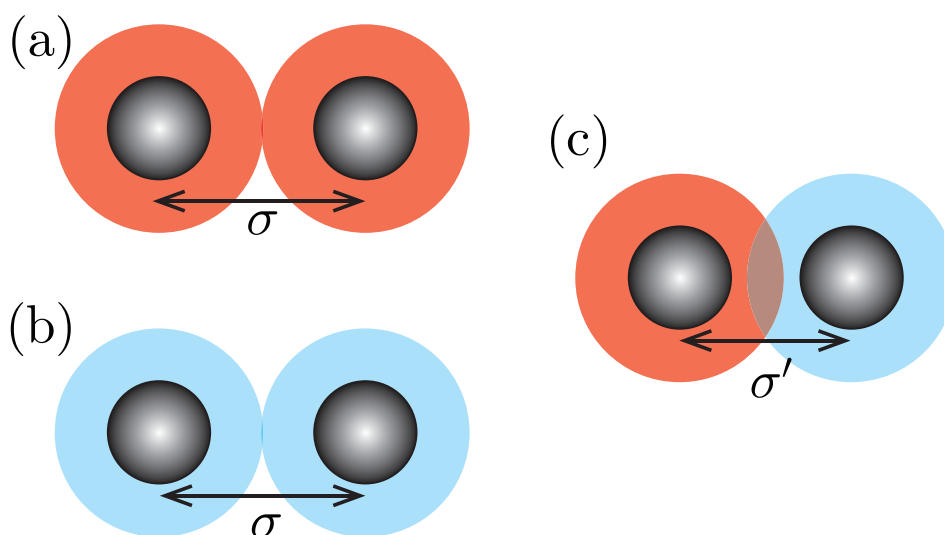


Fig. 1. (color online) Schematic figures indicating the interactions between two types of particles. Each particle consists of a hard sphere covered with DNA strands. (a) and (b) When two particles are of the same type and the distance between them is smaller than σ , the particles are repulsive, and (c) when the types of two particles are different, the interaction between them is the short-range attraction given by the Morse potential, which is minimum at σ' .

Obtaining an idea from the particles covered with DNA strands, we consider a two-dimensional binary system. In our simulation, particles are expressed by circles and the interactions between them are isotropic. We assume that the particles are attractive when their types are different (Fig. 1). As the attractive potential between different types of particles, we use the Morse potential given by

$$U(r) = \epsilon \left[1 - \exp\left(-\frac{r - \sigma'}{a}\right) \right]^2, \quad (1)$$

where ϵ , σ' , and a represent the interaction strength, the distance giving the potential minimum, and the interaction range, respectively. r is the distance between two particles. The particles are repulsive when $r < \sigma'$ and attractive when $r > \sigma'$. The range of attraction becomes small when we set a to be small. For the same type of particles, the interaction potential is given by

$$U(r) = \begin{cases} \epsilon \left[1 - \exp\left(-\frac{r-\sigma}{a}\right) \right]^2 & (r < \sigma), \\ 0 & (r > \sigma). \end{cases} \quad (2)$$

The particles are repulsive when $r < \sigma$ and do not interact with each other when $r > \sigma$. To focus on the difference between σ and σ' , we assume that ϵ and a are the same in Eqs. (1) and (2).

Since particles migrate on a lipid bilayer in an experiment,¹⁷⁾ the particles probably receive both thermal noise and friction from the lipid bilayer. Thus, we consider the particles moving in a two-dimensional system with both thermal noise and friction. When the friction is large, the velocity of the i th particle is given by

$$\frac{d\mathbf{r}_i}{dt} = \frac{1}{\zeta} \left(- \sum_{i \neq j} \nabla U(r_{ij}) + \mathbf{F}_i^{\text{B}}(t) \right), \quad (3)$$

where ζ is the frictional coefficient, \mathbf{r}_i is the position of the i th particle, and $r_{ij} = |\mathbf{r}_i - \mathbf{r}_j|$. The thermal noise $\mathbf{F}_i^{\text{B}}(t)$ satisfies the following relations:

$$\langle \mathbf{F}_i^{\text{B}}(t) \rangle = \mathbf{0}, \quad (4)$$

$$\langle \mathbf{F}_i^{\text{B}}(t) \cdot \mathbf{F}_j^{\text{B}}(t') \rangle = 4\zeta k_{\text{B}} T \delta_{ij} \delta(t - t'), \quad (5)$$

where k_{B} is the Boltzmann constant and T is temperature. A simple differential equation of Eq. (3) is given by³⁸⁾

$$\mathbf{r}_i(t + \Delta t) = \mathbf{r}_i(t) - \frac{1}{\zeta} \sum_{i \neq j} \nabla U(r_{ij}) \Delta t + \Delta \mathbf{r}_i^{\text{B}}(t). \quad (6)$$

$\Delta \mathbf{r}_i^{\text{B}}$ is the displacement caused by the thermal noise, which satisfies

$$\langle \Delta \mathbf{r}_i^{\text{B}}(t) \rangle = \mathbf{0}, \quad (7)$$

$$\langle \Delta \mathbf{r}_i^{\text{B}}(t) \cdot \Delta \mathbf{r}_j^{\text{B}}(t') \rangle = \frac{4k_{\text{B}} T \Delta t}{\zeta} \delta_{ij} \delta(t - t'). \quad (8)$$

In our simulation, we set parameters for the two-dimensional structures to be easily formed in a short time and to be stable for thermal fluctuation. We set parameters as $\sigma = 1$, $a = 0.05$, $\epsilon/\zeta a = 40$, $k_{\text{B}} T/\zeta = 0.1$, and $\Delta t = 10^{-6}$. The attractive range is

sufficiently short because a is much shorter than σ . Since $\epsilon\sigma/(ak_{\text{B}}T) \gg 1$, the thermal noise is sufficiently small for the particles to be ordered. In our simulation, we investigate how two-dimensional structures formed by the particles depend on σ'/σ .

3. Results

In our simulation, we set the numbers of two types of particles to be the same. The total number of particles N_{a} is 1000. Since we want to study the properties of the bulk structure, we set the area fraction ϕ to be large. When we estimate ϕ , we regard the particles as the circles whose diameter is σ . Since we set ϕ to 0.6, the system size L is given by $L = (N_{\text{a}}\pi\sigma^2/4\phi)^{1/2} = 36.18$. We initially locate the particles at random. To make the particle density uniform with small fluctuation, we use Eq. (2) as the potential between particles and move all the particles for a long time. Then, we start simulations with the potentials given by Eqs (1) and (2).

Figure 2 shows the snapshots of the structures appearing in a late stage. The structure is obscure when $\sigma'/\sigma = 1$ [Fig. 2(a)]. It becomes obvious when $\sigma'/\sigma = 0.8$ [Fig. 2(b)]: a square lattice is formed in the system. The lattice structure changes with decreasing σ'/σ . A honeycomb structure is formed when $\sigma'/\sigma = 0.6$ [Fig. 2(c)]. No lattice structure is formed, but short string-shaped clusters appear when $\sigma'/\sigma = 0.5$ [Fig. 2(d)].

To distinguish the structures more qualitatively, we introduce a parameter $\psi_{\mathbf{k}}(l)$ defined as

$$\psi_{\mathbf{k}}(l) = \frac{1}{N_{\text{n}}(l)} \left| \sum_m e^{ik\theta_{lm}} \right|, \quad (9)$$

where $N_{\text{n}}(l)$ is the number of the nearest-neighboring particles for the l th particle and θ_{lm} is the angle between \mathbf{r}_{lm} and the x -direction. Figure 3 shows the radial distribution function $g(r)$ for $\sigma'/\sigma = 0.6$. The definition of $g(r)$ is given by

$$g(r) = \left\langle \frac{1}{N_{\text{a}}} \sum_i \frac{n_i(r)}{2\pi r \delta r} \right\rangle, \quad (10)$$

where $n_i(r)$ is the number of particles whose distance from the i th particle is between r and $r + \delta r$, and $\langle \dots \rangle$ represents the ensemble average. The data are averaged over 10 individual runs. We use $\delta r = 10^{-2}$ when we calculate $g(r)$. The first peak, which appears when r is about 0.6, is sufficiently sharp and separated from the second peak appearing when r is about 1. Since this tendency of the formation of the sharp and isolated first peak does not depend on σ'/σ , we easily distinguish the nearest neighbors

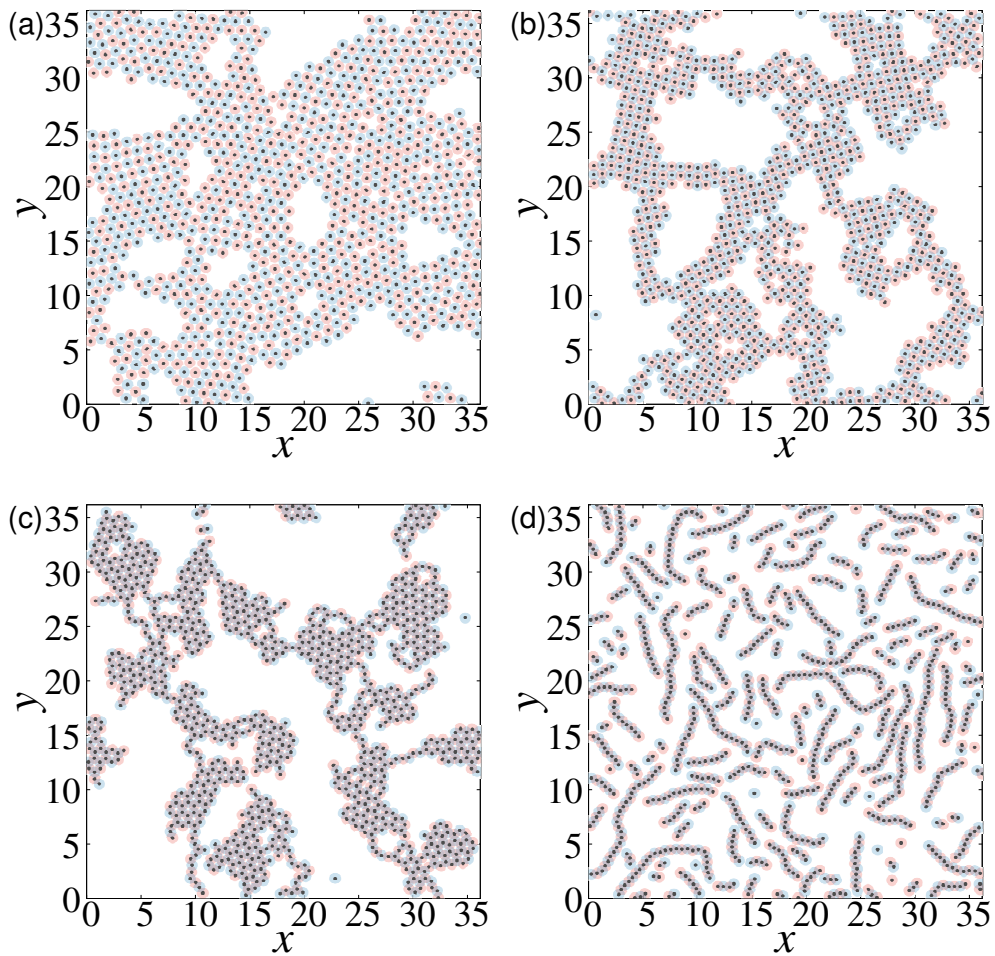


Fig. 2. (color online) Snapshots of structures appearing in a late stage. σ'/σ is set to (a) 1, (b) 0.8, (c) 0.6, and (d) 0.5. Time is (a) 4000, (b) and (c) 1000, and (d) 2000. The types of particles are distinguished by the difference in colors. To show the lattice structures clearly, we draw a black circle at the center of each particle.

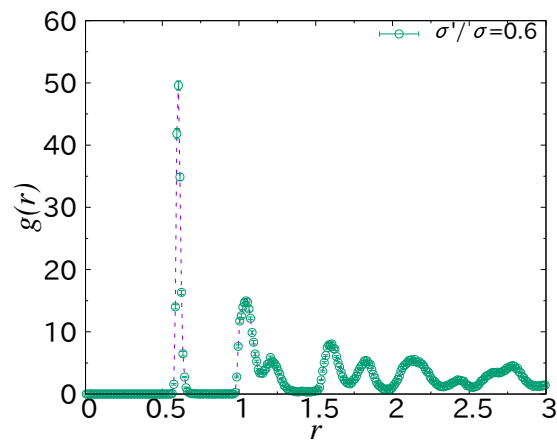


Fig. 3. (color online) Radial distribution function $g(r)$ in the case of $\sigma'/\sigma = 0.6$. The data are averaged over 10 individual runs.

for all σ'/σ 's.

$\psi_k(l)$ shows the local k -fold rotational symmetry around the l th particle. We estimate $\psi_k(l)$ for $k = 2, 3, 4$, and 6 . When the l th particle has the perfect k -fold rotational order, $\psi_k(l) = 1$. $\psi_k(l)$ decreases with decreasing quality of symmetry, and $\psi_k(l) = 0$ when the particles do not have the k -fold rotational symmetry at all. $\psi_k(l)$ does not show the symmetry correctly when the number of the nearest neighbors is too small. Thus, we calculate $\psi_6(l)$ when $N_n(l) \geq 4$. For $\psi_4(l)$, $\psi_3(l)$, and $\psi_2(l)$, we estimate them when $N_n(l) \geq 2$. Probably, particles do not have the perfect rotational order because of thermal fluctuation. Thus, we consider that the l th particle has the k -fold rotational symmetry when $\psi_k(l) > 0.7$. We count the number of particles that have the k -fold rotational symmetry, n_k , and define the density of the particles having the k -fold symmetry, ρ_k , as n_k/N_a .

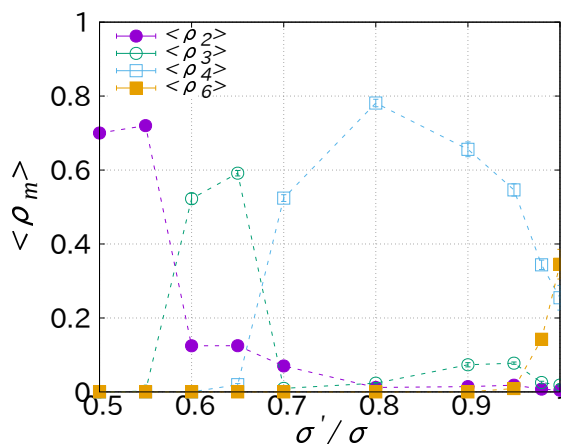


Fig. 4. (color online) Dependences of $\langle \rho_2 \rangle$, $\langle \rho_3 \rangle$, $\langle \rho_4 \rangle$, and $\langle \rho_6 \rangle$ on σ'/σ . The data are averaged over 10 individual runs.

Figure 4 shows the dependences of $\langle \rho_2 \rangle$, $\langle \rho_3 \rangle$, $\langle \rho_4 \rangle$, and $\langle \rho_6 \rangle$ on σ'/σ . When $\sigma'/\sigma = 1$, both $\langle \rho_6 \rangle$ and $\langle \rho_4 \rangle$ are finite, and the other parameters are negligibly small, which probably shows that a mixture of both triangular and square lattices is formed when $\sigma' = \sigma$. Since $\langle \rho_6 \rangle$ is larger than $\langle \rho_4 \rangle$, the number of the triangular lattice may be larger than that of the square lattice. In Fig. 2(a), the formation of both square and triangular lattices is unclear. Thus, we show how the particles satisfying $\psi_4 > 0.7$ and $\psi_6 > 0.7$ are located in Fig. 5. In the snapshot, the blue and red circles represent the particles that satisfy $\psi_4 > 0.7$ and $\psi_6 > 0.7$, respectively. Both the clusters formed by the triangular lattice and those formed by the square lattice are present. The cluster size with the

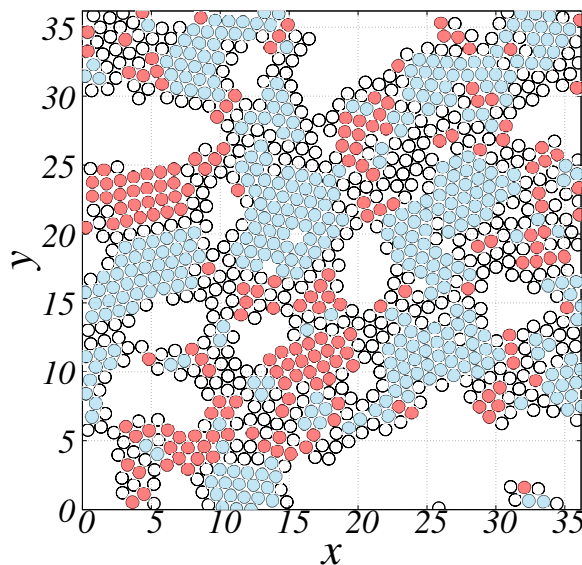


Fig. 5. (color online) Snapshot of system with $\sigma'/\sigma = 1$ at $t = 4000$. The red and blue circles represent the particles that satisfy $\psi_4 > 0.7$ and $\psi_6 > 0.7$, respectively.

triangular lattice seems to be larger than that with the square lattice.

When $\sigma'/\sigma < 0.95$, one parameter is large and the other parameters are negligibly small. The result shows that one structure occupies the system and the structure changes with decreasing σ'/σ . From Fig. 4, we think that the structure formed in the system is the square lattice when $0.65 < \sigma'/\sigma < 0.95$, the honey-comb lattice when $0.55 < \sigma'/\sigma < 0.65$, and the string-shaped clusters whose direction is not in order when $\sigma'/\sigma < 0.55$, which is consistent with the snapshots in Fig. 2.

The appearance of the mixture of both triangular and square lattices in the case of large σ'/σ and the formation of clusters in the case of small σ'/σ are different from our previous study.³⁶⁾ Since we suspect that the formation of the mixture of the two structures in the case of a large σ'/σ is because the system has not yet reached equilibrium, we investigate the time evolution of both $\langle \rho_4 \rangle$ and $\langle \rho_6 \rangle$ (Fig. 6). The particles having the four-fold symmetry appear mainly in an early stage. Then, when large clusters are formed, the particles in the clusters have the six-fold symmetry. $\langle \rho_6 \rangle$ increases rapidly and becomes larger than $\langle \rho_4 \rangle$. Although $\langle \rho_6 \rangle$ is saturated more slowly than $\langle \rho_4 \rangle$, both $\langle \rho_4 \rangle$ and $\langle \rho_6 \rangle$ are finally saturated. Thus, the mixture of the two lattices is in the equilibrium state. In our simulation, $\langle \rho_6 \rangle$ is larger than $\langle \rho_4 \rangle$ in the last stage when $\phi = 0.6$ [Fig. 6(a)]. However, $\langle \rho_4 \rangle$ is always larger than $\langle \rho_6 \rangle$ although the simulation time is longer than that in Fig. 6(a) when ϕ decreases and is given by 0.2 [Fig. 6(b)].

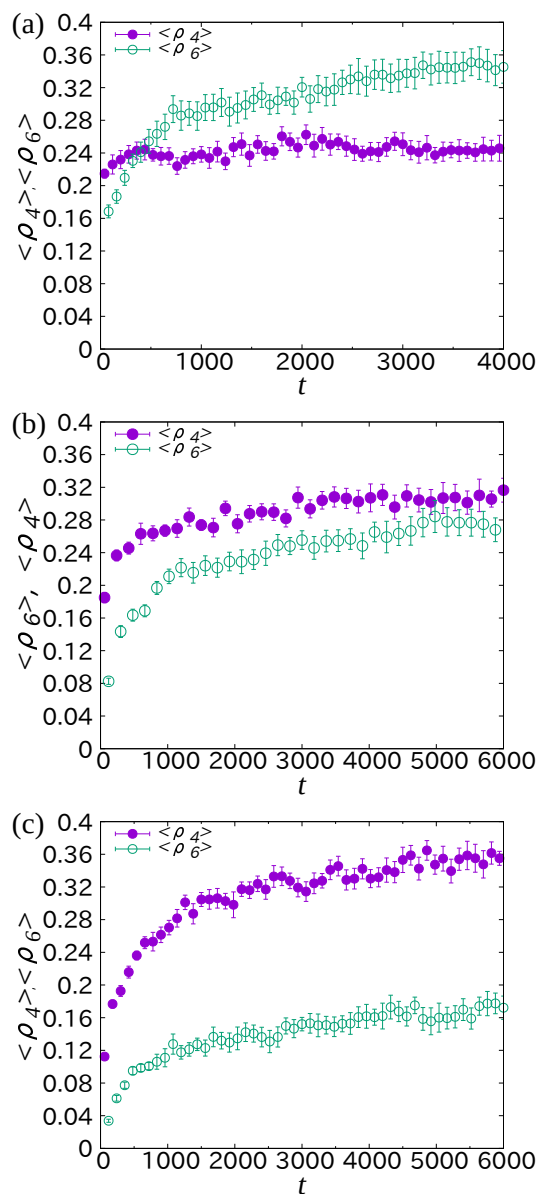


Fig. 6. (color online) Time evolution of $\langle \rho_4 \rangle$ and $\langle \rho_6 \rangle$ in the case of $\sigma'/\sigma = 1$. The red squares and blue triangles represent $\langle \rho_4 \rangle$ and $\langle \rho_6 \rangle$, respectively. The data are averaged over 10 individual runs. ϕ is (a) 0.6, (b) 0.2, and (c) 0.1.

The difference between $\langle \rho_4 \rangle$ and $\langle \rho_6 \rangle$ becomes large when $\phi = 0.1$ [Fig. 6(c)]. Thus, the saturated values of $\langle \rho_6 \rangle$ and $\langle \rho_4 \rangle$ depend on ϕ . The formation of large clusters is difficult when ϕ is small, which probably makes $\langle \rho_6 \rangle$ smaller than $\langle \rho_4 \rangle$.

Since we set the temperature to be much smaller than ϵ , the reason why both square and triangular lattices coexist in the case of a large σ'/σ is understood qualitatively when we consider the energy gains by forming these lattices. In our model, a particle interacts with its nearest neighbor when their types are different. Thus, the energy gain

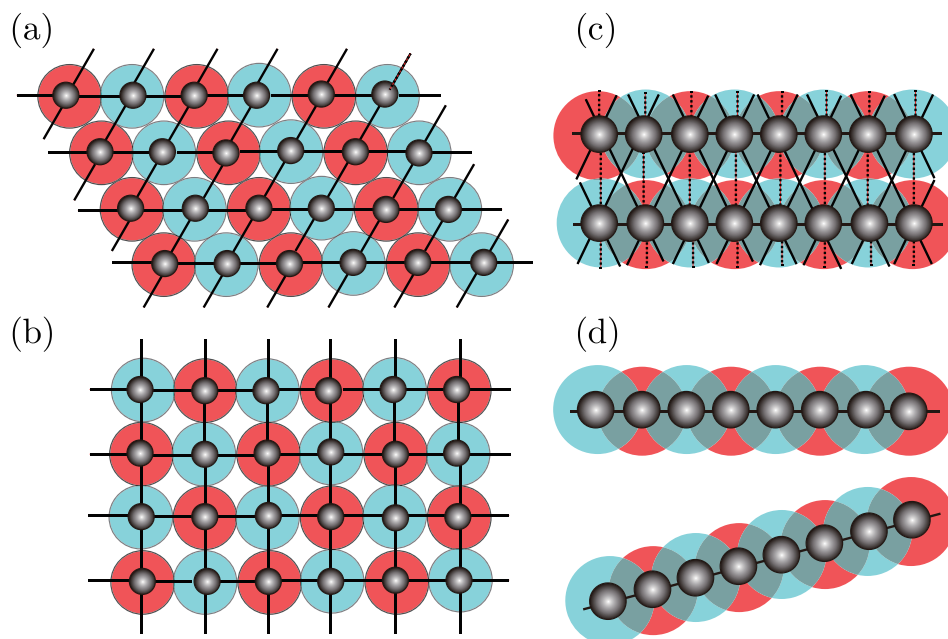


Fig. 7. (color online) Interactions in (a) a triangular lattice, (b) a square lattice, (c) a rectangular lattice in our previous study,³⁶⁾ and (d) string-shaped clusters. In Figs. 7(a), 7(b), and 7(d), the solid lines connecting the centers of the two particles represent the attraction between the nearest neighbors. In Fig. 7(c), the attraction between the second nearest neighbors is shown as dotted lines. The interaction between the third nearest neighbors, which is as large as that between the nearest neighbors, is also drawn by a solid line.

by forming the square lattice [Fig 7(b)] is the same as that by forming the triangular lattice [Fig 7(a)]. The particles are initially located randomly in the system. Since the packing ratio of the triangular lattice is larger than that of the square lattice, the square lattice is formed more easily than the triangular lattice. Thus, it is mainly the square lattice that is formed in the initial stage. Then, the formation of the triangular lattice starts. In our previous study,³⁶⁾ the square lattice is not formed when $\sigma'/\sigma = 1$. Since particles are attractive when their types are the same, the energy gain by forming the triangular lattice is larger than that by forming the square lattice in that study.³⁶⁾ Here, we assume that a long-range attraction is present only between the different types of particles. For example, we use the LJ potential for the different types of particles and the Weeks–Chandler–Anderson (WCA) potential,³⁹⁾ which is the potential formed by the repulsive part of LJ potential, for the same types of particles. The energy gain by forming a triangular lattice is larger than that by forming a square lattice because of the effect of the second nearest interaction when $\sigma'/\sigma = 1$.

The attraction from the second nearest neighbors also affects the formation of struc-

ture when $\sigma'/\sigma \leq 0.6$. In our previous study,³⁶⁾ a rectangular lattice, whose two sides are about σ and σ' , is formed when $0.475 < \sigma'/\sigma < 0.625$. The nearest neighbors and the second nearest neighbors are the different types of particles and the third nearest neighbors are the same types of particles. In that model, the interaction potential is given by the LJ potential. Although the distances giving the potential minimum are given by $2^{1/6}\sigma$ for the same type of particles and $2^{1/6}\sigma'$ for the different types of particles, the interaction strength does not depend on the particle type. Thus, the attraction from the third nearest neighbors is as large as that from the nearest neighbors. These attractions are the main effects on the formation of the rectangular lattice. In addition to these attractions, the attraction from the second nearest neighbors also supports the formation of the rectangular lattice [Fig. 7(c)]. Here, on the other hand, we neglect the attraction between the same type of particles. Thus, the attractions from the third nearest neighbors in Fig. 7(c) are eliminated. Since the interaction between the different types of particles is short-range, the support from the second nearest neighbors is also absent. Since the particles interact with only the nearest neighbors, the string-shaped clusters [Fig. 7(d)] are formed as shown in Fig. 2(d).

4. Summary

In this paper, obtaining an idea from the two-dimensional structures formed by DNA nanoparticles,^{17, 18)} we carried out Brownian dynamics simulations and studied the two-dimensional structures formed in a binary system. We assumed that the different types of particles are attractive with the Morse potential, which is minimum when their distance is σ' , and the same type of particles are repulsive when their distance is smaller than σ . We investigated how the structures formed by the two types of particles depend on σ'/σ . When the difference between σ' and σ is sufficiently small, both square and triangular lattices coexist. The structure changes with decreasing σ'/σ : the square and honeycomb lattices are formed when $0.65 < \sigma'/\sigma < 0.95$ and $0.55 < \sigma'/\sigma < 0.65$, respectively. When $\sigma'/\sigma < 0.55$, the string-shaped clusters are formed.

Comparison of the results with our previous study,³⁶⁾ shows that the coexistence of the two lattices in the case of large σ'/σ and the formation of string-shaped clusters in the case of small σ'/σ are different: in the previous study, the triangular lattice is formed in the case of large σ'/σ and the rectangular lattice is formed in the case of small σ'/σ . The differences between the model in this study and the previous model³⁶⁾ are the absence of the attraction between the same types of particles and the short range

interaction. Both differences are important for the coexistence of these two lattices in the case of large σ'/σ and string-shaped clusters in the case of small σ'/σ . On the other hand, although the range of σ'/σ is slightly different from that in Ref. 36, both square and honeycomb lattices are formed, which shows that the formation of these structures mainly depends on the nearest neighbors' number determined by σ' .

In an experiment,¹⁷⁾ the lattice structure is changed from a triangular lattice to a square lattice by controlling the magnesium ion density. It is unclear how the effect of the magnesium ion should be expressed in our potential. In our simulation, a honeycomb lattice is formed when $\sigma'/\sigma = 0.6$ [Fig. 2(c)]. In this case, the lattice constant a is given by $a = \sigma'/\sigma = 0.6$ as shown in Fig. 3. Since the square lattice is formed when $0.65 < \sigma'/\sigma < 0.95$, the lattice constant of the square lattice is given by $0.65 < \sigma'/\sigma < 0.95$. Thus, the lattice distance in the triangular lattice, which is obtained in the case of $\sigma'/\sigma > 0.95$, is larger than that in the square lattice, which agrees with the experiment.¹⁷⁾ However, the coexistence of the two structures was not observed in the experiment.¹⁷⁾ Thus, the interaction in the experiment¹⁷⁾ is probably closer to that used in our previous study³⁶⁾ than in this paper: the attraction may be short-range, but the attraction from the same types of particles is probably negligible.

Acknowledgement

The author thanks H. Katsuno for his valuable comments. This work was supported by JSPS KAKENHI under Grant Nos. JP16K05470, JP18K04960, and JP18H03839, and Joint Research Program of the Institute of Low Temperature Science, Hokkaido University under Grant No. 18G019.

References

- 1) J. C. Crocker, *Nature (London)* **451**, 528 (2008).
- 2) S. Y. Park, A. K. R. Lytton-Jean, B. Lee, S. Weigand, and G. C. Schatz, *Nature (London)* **451**, 553 (2008).
- 3) D. Nykypanchuk, M. M. Maye, D. v. d. Lelie, and O. Grang, *Nature (London)* **451**, 549 (2008).
- 4) H. Xiong, D. v.d. Lelie, and O. Grang, *Phys. Rev. Lett.* **102**, 015504 (2009).
- 5) W. B. Rogers and J. C. Croker, *Proc. Natl. Acad. Sci. USA* **38**, 15687 (2011).
- 6) C. Zhang, C. R. J. Macfarlane, K. L. Young, C. H. J. Choi, L. Hao, E. Auyyeung, G. Liu, X. Zhou, and C. A. Mirkin, *Nat. Mater.* **12**, 741 (2013).
- 7) M. R. Jones, R. J. Macfarlane, B. Lee, Z. Jian, K. L. Young, A. J. Senesi, and A. C. Mirkin, *Nat. Mater.* **9**, 913 (2010).
- 8) P. Cigler, K. R. Lytton-Jean, D. G. Anderson, M. G. Finn, and S. Y. Park, *Nat. Mater.* **9**, 918 (2010).
- 9) R. J. Macfarlane, B. Lee, M. R. Jones, N. Harris, G. C. Schatz, and C. A. Mirkin, *Science* **334**, 204 (2011).
- 10) C. A. Mirkin, *MRS Bull.* **35**, 532 (2010).
- 11) S. T. Han, Y. Zhou, Z. X. Xu, L. B. Huang, X. B. Yang, and V. A. L. Roy, *Adv. Mater.* **24**, 3556 (2012).
- 12) F. Frederix, J. M. Friedt, K. H. Choi, W. Laureyn, A. Campitelli, D. Mondelaers, G. Maes, and G. Borghs, *Anal. Chem.* **75**, 6894 (2003).
- 13) T. Endo, K. Kerman, N. Nagatani, H. M. Hiepa, D. K. Kim, Y. Yonezawa, K. Nakano, and E. Tamiya, *Anal. Chem.* **78**, 6465 (2006).
- 14) D. S. Sebba, J. J. Mock, D. R. Smith, T. H. LaBean, and A. A. Lazarides, *Nano Lett.* **8**, 1803 (2008).
- 15) D. K. Kim, S. M. Yoo, T. J. Park, H. Yoshikawa, E. Tamiya, J. Y. Park, and S. Y. Lee, *Anal. Chem.* **83**, 6215 (2011).
- 16) S. Srivastava, D. Nykypanchuk, M. Fukuto, J. D. Halverson, A. V. Tkachenko, K. G. Yager, and O. Gang, *J. Am. Chem. Soc.* **136**, 8323 (2014).
- 17) T. Isogai, E. Akada, S. Nakada, N. Yoshida, R. Tero, S. Harada, T. Ujihara, and M. Tagawa, *Jpn. J. Appl. Phys.* **55**, 03DF11 (2016).
- 18) T. Isogai, A. Piednoir, E. Akada, Y. Akahoshi, R. Tero, S. Harada, T. Ujihara, and M. Tagawa, *J. Cryst. Growth* **494**, 401 (2014).

- 19) J. Duguid, V. A. Bloomfield, J. Benevides, and G. J. Thomas Jr., *Biophys J.* **65**, 1916 (1993).
- 20) T. K. Chiu and R. E. Dickerson, *J. Mol. Biol.* **301**, 915 (2000).
- 21) S. R. Walter, K. L. Young, J. G. Holland, R. L. Gieseck, C. A. Mirkin, and F. M. Geiger, *J. Am. Chem. Soc.* **135**, 17339 (2013).
- 22) S. Nakano, M. Fujimoto, H. Hara, and M. Sugimoto, *Nucleic Acids. Res.* **27**, 2957 (1999).
- 23) R. Owczarzy, B. G. Moreira, Y. You, M. A. Behlke, and J. A. Walder, *Biochemistry* **47**, 5336 (2008).
- 24) L. Largo, F. Starr, and F. Sciortino, *Langmuir* **23**, 5896 (2007).
- 25) W. Dai, C. W. Hsu, F. Starr, and F. Sciortino, *Langmuir* **26**, 3601 (2010).
- 26) C. Knorowski, S. Burleigh, and A. Travesser, *Phys. Rev. Lett.* **106**, 215501 (2011).
- 27) T. Li, R. Sknepnek, and M. Cruz, *J. Am. Chem. Soc.* **135**, 8535 (2013).
- 28) A. Tkachenko, *Phys. Rev. Lett.* **89**, 148303 (2011).
- 29) M. J. Vlot, H. E. A. Huitema, A. de Vooy, and J. P. van der Eerden, *J. Chem. Phys.* **107**, 4345 (1997).
- 30) M. J. Vlot and J. P. van der Eerden, *J. Chem. Phys.* **109**, 6043 (1998).
- 31) L. D. Michele, F. Varrato, J. Kotar, S. N. Nathan, G. Foffi, and E. Eiser, *Nat. Commun.* **4**, 2007 (2013).
- 32) H. Pattabhiraman and M. Dijkstra, *J. Chem. Phys.* **147**, 104902 (2017).
- 33) H. Pattabhiraman, A. P. Gantapara, and M. Dijkstra, *J. Chem. Phys.* **143**, 164905 (2015).
- 34) H. Pattabhiraman and M. Dijkstra, *Soft Matter* **143**, 4418 (2017).
- 35) T. Dotera, T. Oshiro, and P. Ziherl, *Nature* **208**, 506 (2014).
- 36) H. Katsuno, Y. Maegawa, and M. Sato, *J. Phys. Soc. Jpn.* **85**, 074605 (2016).
- 37) K. Tanaka, H. Katsuno, and M. Sato, *Jpn. J. Appl. Phys.* **55**, 075001 (2017).
- 38) D. L. Ermak, *J. Chem. Phys.* **62**, 4189 (1975).
- 39) J. D. Weeks, D. Chandler, and H. C. Anderson, *J. Chem. Phys.* **54**, 5237 (1971).